Analysis of a ^{207}Bi spectrum measured with a Hamamatsu photo diode, a TSH310 based preamp, and the HETI IRENA

Stephan I. Böttcher

2011-06-01, Revision 649

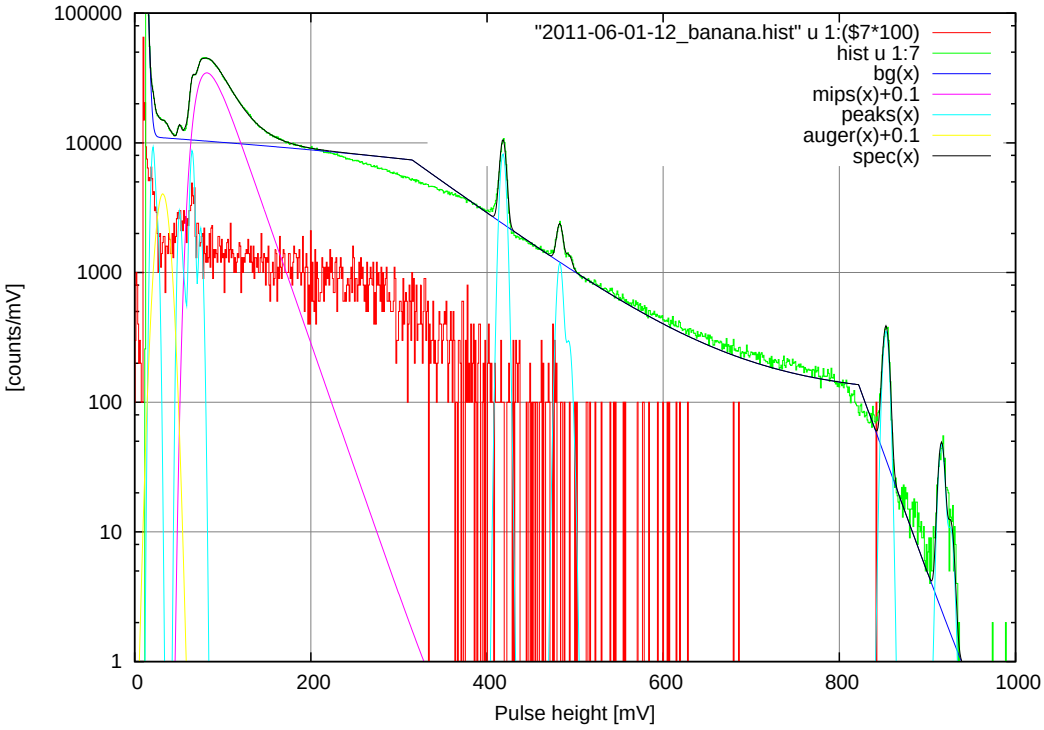

Figure 1: ^{207}Bi spectrum in 300 μm Silicon with backscatter.

Contents

List of Figures

List of Tables

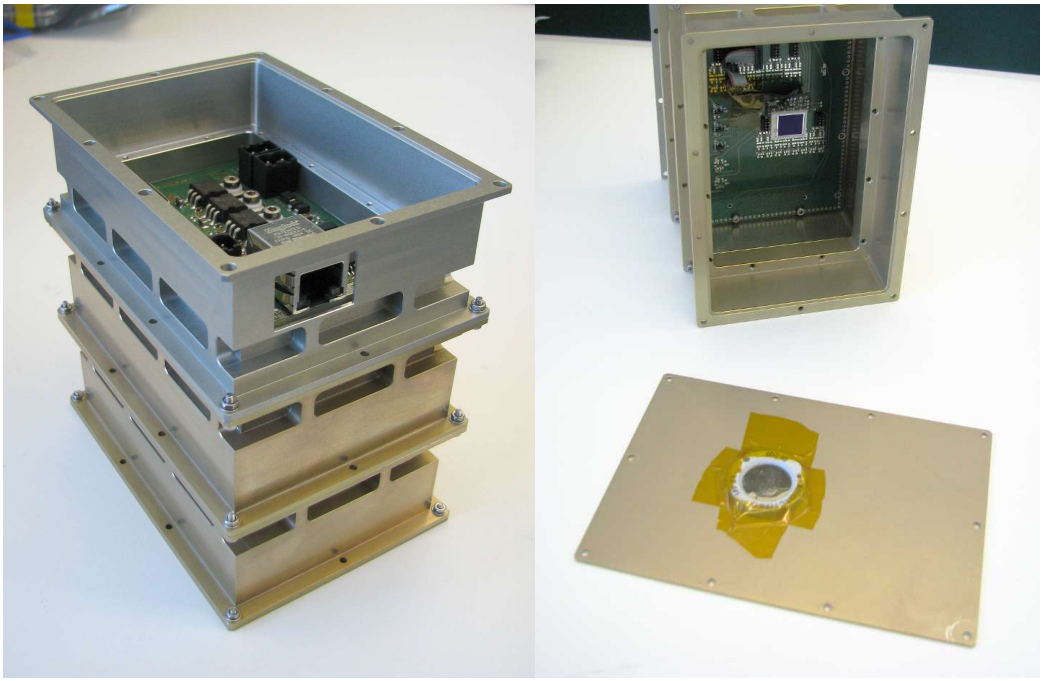

Figure 2: IRENA stack and source.

1 Setup

Preamp number 9, as tested by Martin Kruse for SOLO-HET is connected to channel 4/5 (L/H) of the HETI IRENA, via a VIRENA-IFC board. The IRENA shaping time constant is 1 μs.

A Hamamatsu photodiode, 1 cm^2, no epoxy window, is directly soldered to the preamp. The preamp is fixed to the VIRENA-IFC board with Capton tape, the detector facing away from the board. A third module housing is attached to the IRENA, with the source taped to the cover plate a few centimeters distance from the detector. The GSE power board is used, readout via USB to falbala. The setup operated in office air.

1.1 IRENA

The IRENA is an 18-channel, 3 MSPS, 12-bit, digital acquisition system. The FPGA logic is inherited from the DIRENA. In the DIRENA design, the FPGA was connected via parallel port to a PC. The IRENA has an additional ARM 7 microcontroller which connects to the PC via USB.

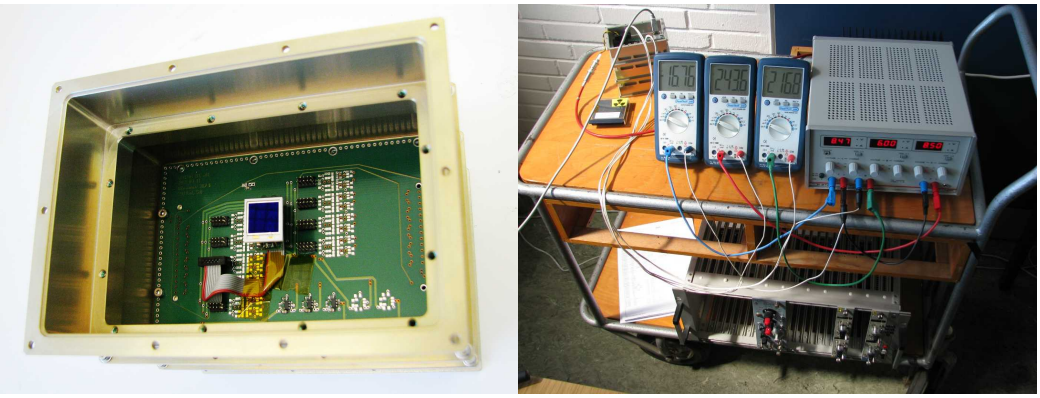

Figure 3: Photodiode (left). Complete Setup (right).

The IRENA has included one-zero/one-pole shaping amplifiers directly next to the ADCs, with alternating high (×15) and low (×1) gain to support nine dual-gain input channels. These shapers also isolate the clock-feed-through from the ADCs from the frontend.

Fig. 2 shows the stack of three module housings, and how the source is taped to the bottom cover plate. Fig. 3 gives a closer view on the photodiode, with the preamp attached and taped to the interface board. On the right picture is the complete setup, with a NIM crate for the detector bias supply (−50 V), a lab power supply, current meters, and the IRENA.

1.2 Power board

The IRENA PCB with ADCs, FPGA, ARM 7, is supplemented with a power regulator board. For this test we used the GSE board that is usually only used for smoke tests of new xRENA boards, of for flashing firmware. This board does not provide the full isolation of the different analog and digital power supplies, as a production power board is supposed to do.

1.3 Charge sensitive pre-amplifier

In place of a preamp board, this test employs a simple interface board VIRENA-IFC, with individual connectors for preamps of the nine channels.

A single channels is used, with a single preamp isolated from a HAMA-PREAMPS board. That preamp was tested as number 9 by Martin Kruse for evaluating the design for Solar Orbiter EPD-HET.

The preamp schematic is show in Fig. 4. The buffer amplifier is a TSH310 current feedback amplifier, with high bandwidth and extremely low power

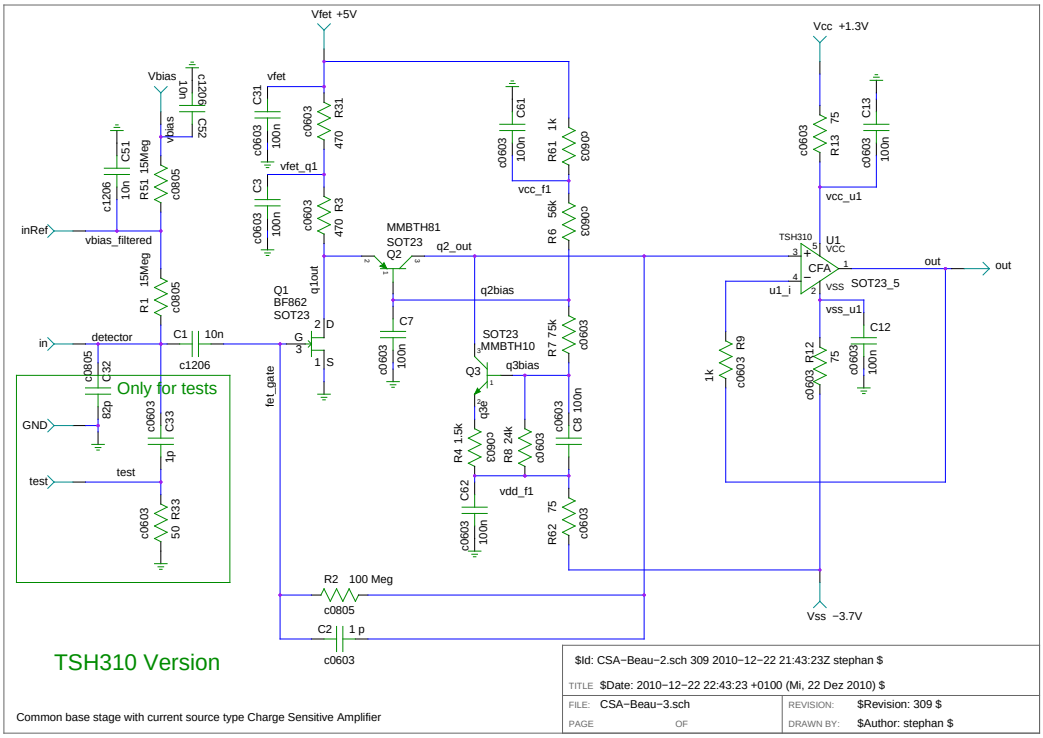

Figure 4: Preamp schematic.

consumption. We used AD8005 devices before, which can operate at $\pm 5\,\mathrm{V}$, but they do not come qualified for space flight.

1.4 Pulse height and phase reconstruction

The shaper outputs are sampled by ADCs at 3 MSPS. The last 64 samples of each channel are stored in a ring buffer. After each sample, a pulse height and phase reconstruction is started, based on a subset of up to 16 samples in the ring buffer. $s_i,\ i = 0 \ldots 15$ shall be the selected set of samples, with s_0 being the last sample read by the ADC, and the others at fixed times before that last sample. The pulse height A and the phase parameter B are then computed as a linear combinationa of these samples, with coefficients a_i and b_i

$$A = \sum_{i=0}^{15} a_i s_i, \tag{1}$$

$$B = \sum_{i=0}^{15} b_i s_i. \tag{2}$$

To be independent of the signal pedestal, the sum of the coefficients must be zero

$$\sum_{i=0}^{15} a_i = \sum_{i=0}^{15} b_i = 0. \tag{3}$$

The values of A for successive times are compared, to find local maxima. I.e., when the middle of three successive pulse heights A is the largest of the three, that value is further compared to a trigger threshold, and if the threshold is exceeded, an event triggers. In that case, The A and B from all channels are saved. Optionally, a number of samples s_i from the ring buffer can be saved as well.

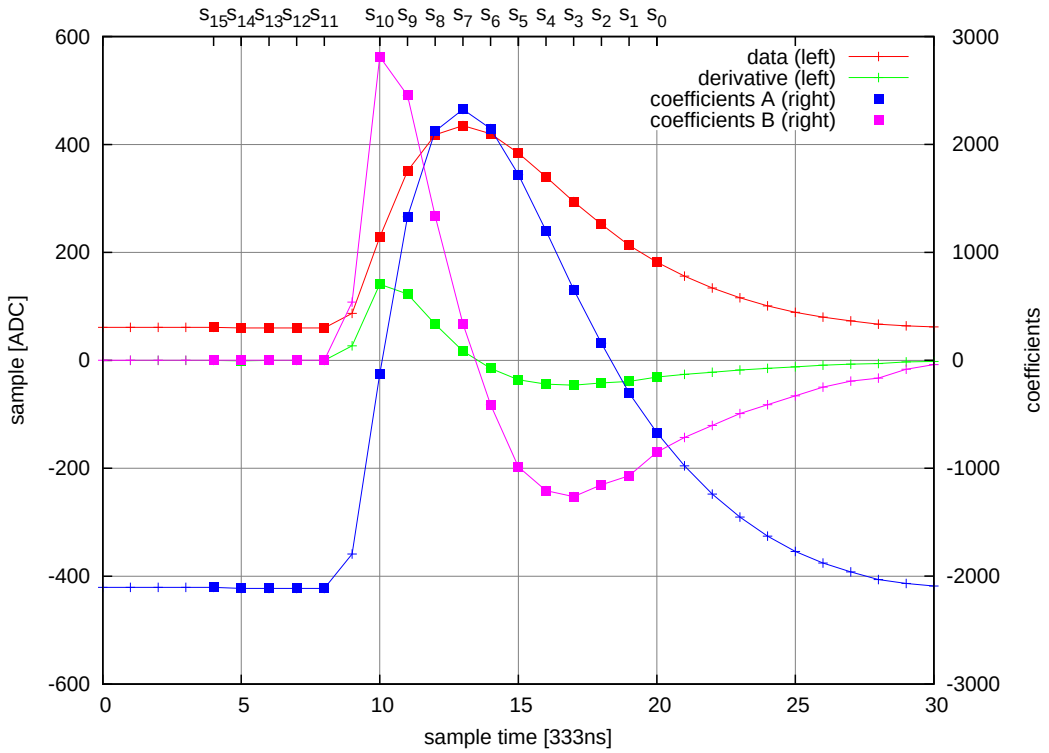

Figure 5: Pulse shape and DIRENA coefficients.

1.4.1 Obtaining DIRENA coefficients

To obtain good coefficients a_i and b_i, enable saving samples, and run with a pulse generator or cosmic muons. In that data set a large pulse is selected and analysed, e.g., with a spreadsheet program. Fig. 5 shows the coefficients used in this analysis and the pulse shape they are based on. In red are the sample

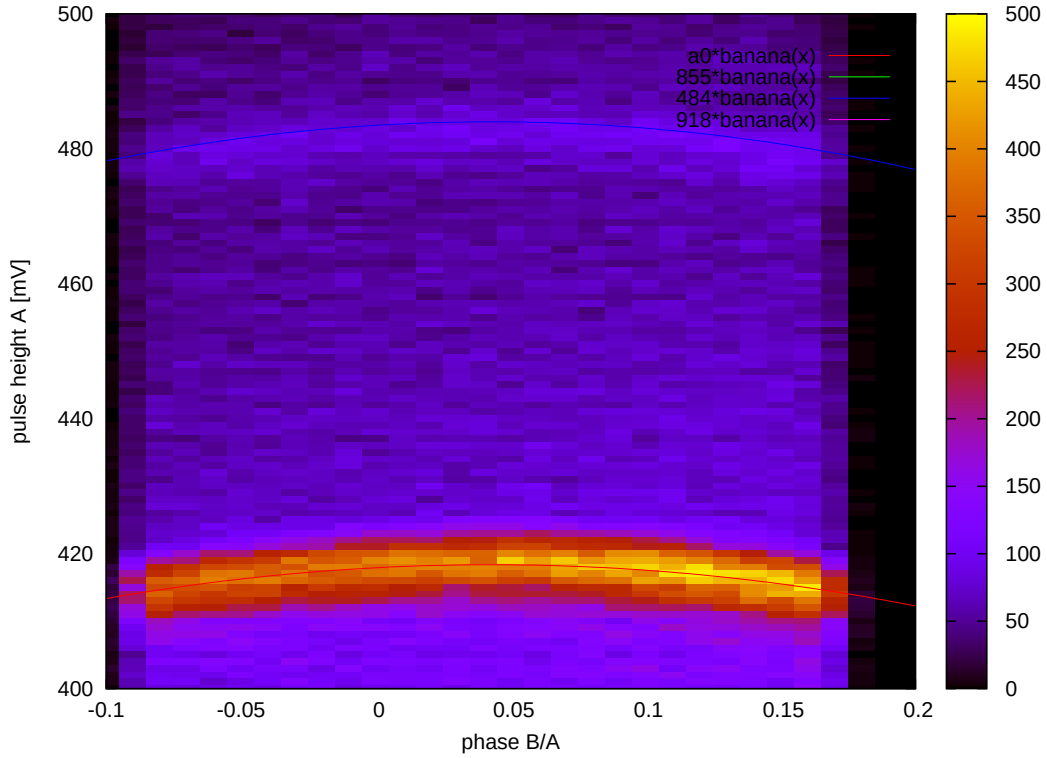

Figure 6: Banana of the 482 keV and 554 keV lines.

data s_i, green are the differences to the previous sample, the derivative, blue are the pulse height coefficients a_i and pink the phase coefficients b_i.

The first step is to select sixteen samples. A balanced number of samples on the top of the peak and on the baseline before the peak, plus a few where the peak is steepest, on both the rising and falling edge.

Next, the pulse shape is offset, so that the average of the selected samples is zero. The coefficents a_i are proportional to the offset samples. The coefficents b_i are proportional to the derivative, but the rising and falling edge are normalized independently, to get a sum of zero.

This analysis has a flaw, because the derivative is shifted by half a sample. The a_i should have been the offset average of two consecutive samples. Well, next time.

1.4.2 Banana correction

The pulse height reading A depends on the phase φ of the ADC clock relative to the signal. The phase is a monotonic function of the normalized B

$$\varphi = f\left(\frac{B}{A}\right) \tag{4}$$

For a constant pulse height, with arbitrary phase, a scatter plot A vs B/A looks like a banana. Fig. 6 shows the banana of the 482 keV line in our spectrum. This banana for the 1 μs-shapers causes 0.5 % loss in resolution, which is recovered by correction

$$A_{\text{corr}} = \frac{A}{1 - 0.6 \cdot \left(\frac{B}{A} - 0.04\right)}. \tag{5}$$

2 The source

Our STEREO ^{207}Bi source, 1 μCi (2003) is used. This source is closed, with very thin foil windows. The prominent emission lines listed by NUDAT 2 are summarized in table 1.

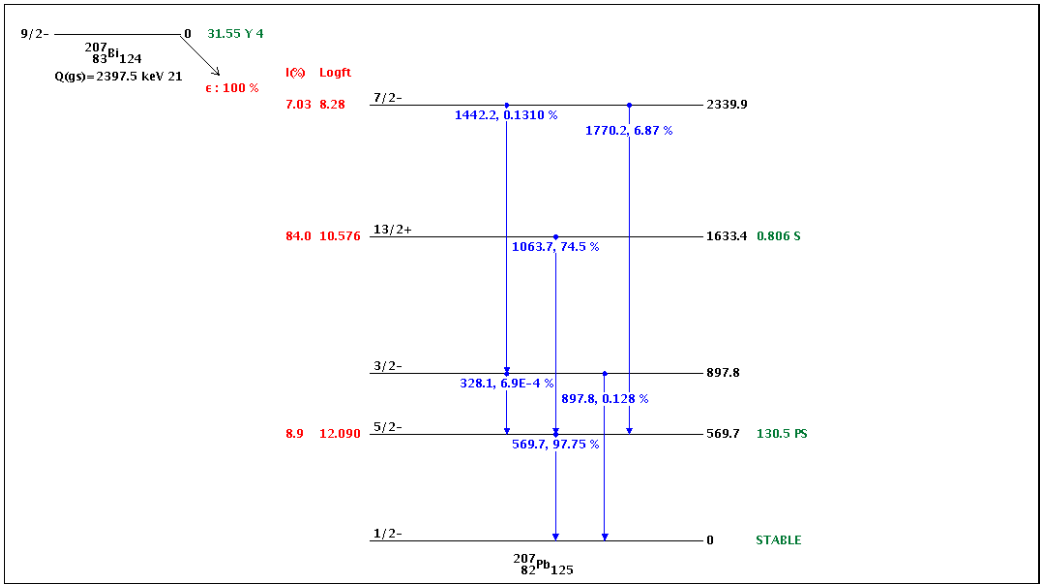

Figure 7: ^{207}Bi decay scheme, NUDAT2.

Table 1: ^{207}Bi emission lines from NuDat2.

Process	Particle	Energy	Intensity
Auger K	e^-	56.7 keV	2.9 %
CE K	e^-	481.6935 keV	1.515 %
CE L	e^-	553.8372 keV	0.438 %
CE M	e^-	565.8473 keV	0.147 %
CE K	e^-	975.651 keV	7.03 %
CE L	e^-	1047.795 keV	1.84 %
CE M	e^-	1059.805 keV	0.54 %
XR	γ	10.6 keV	33.2 %
XR	γ	72.805 keV	21.4 %
XR	γ	74.969 keV	35.7 %
XR	γ	84.45 keV	4.31 %
XR	γ	84.938 keV	8.27 %
XR	γ	87.3 keV	3.02 %
	γ	569.698 keV	97.76 %
	γ	1063.656 keV	74.6 %
	γ	1770.228 keV	6.87 %

2.1 γs

The primary emission of this source are three γ-lines, none of which can be detected with this setup, except if the electrons were shielded from the detector. The background of the red spectrum in Fig. 1 are Compton electron hits. The Compton edge of the 570 keV γ-line can be identified at 394 keV.

2.2 Conversion electrons

The most prominent features of the spectrum originate from conversion electrons. The γ-decays convert with some probability to K-, L-, of M-shell electron emissions.

All of these e^- normally penetrate the detector, contributing to the background. With some small probability those electrons deposit all their energy in the detector. Especially the 976 keV electrons mostly go into the Landau-peak. There are five times more 976 keV electrons than 482 keV electrons, but the probability to get absorbed in 300 μm Silicon is hundred times less, as will be shown below in section 5.1.3.

2.3 X-rays

Two groups of X-rays, at 75 keV and 85 keV can be observed. Each X-ray line appears three times, the photo peak, the Compton backscatter, and the Compton peak.

The 75 keV X-ray gives a photo peak at, well, 75 keV. More prominent is the Compton backscatter peak. The photon passes the detector and scatters in the ceramic/housing/table by 180° back into the detector. The Compton photon energy is

$$E'_\gamma(180°) = \frac{E_\gamma}{1 + \frac{2E_\gamma}{m_e}} = \frac{75\,\mathrm{keV}}{1 + \frac{150\,\mathrm{keV}}{511\,\mathrm{keV}}} = 58\,\mathrm{keV}. \tag{6}$$

When the X-ray scatters inside the detector, we see the Compton electron with energy

$$E_\gamma - E'_\gamma = 75\,\mathrm{keV} - 58\,\mathrm{keV} = 17\,\mathrm{keV}. \tag{7}$$

The 85 keV X-ray is less intensive but still visible at 85 keV, 64 keV, and 21 keV.

2.4 Auger e^-

The source emits Auger electrons at 56 keV. These loose much of their energy in the air between source and detector, but they can be identified.

3 Spectrum

The analyzed run is `2011-06-01-Bi207-13`, which was acquired from 2011-06-01 to 2011-06-03. Also shown is a run `2011-06-06-Bi207-g-26` with the source outside the box, shielded from the detector by the cover plate, made of 1 mm thick Aluminum.

3.1 DIRENA

The DIRENA coefficients were derived from a pulse shape from run `2011-06-01-8`, using a single, large pulse of the muon tail.

The IRENA binary data (`.dat`) is converted to ASCII (`.E`). The banana correction is applied to the data (`_banana.E`).

Only the high gain channel is used in this analysis. The preamp gain is 1/1 pF, the shaper gain is 14.4.

4 Fit

Gnuplot is used to fit the spectrum to a collection of peaks and background models. The models and fits were developed interactively. The script listed in section 9 captures the results of that process. It defines functions for the models, initializes all parameters from a recent fit result, performs the fit, in three major steps (regions), each divided into minor steps. The major steps are

1. The conversion electron lines at 482 keV+,
2. the conversion electron lines at 976 keV+,
3. the low energy X-rays and Landau peak.

The first minor steps of each groups only fit the amplitude parameters, since the spectrum was accumulating counts during analysis. Finally, the remaining parameters of the group are added to the fit, just in case there is an improvement with the new counts.

4.1 Background

The background is modeled piecewise exponential. The Landau region background is linear, plus a steep exponential at the trigger threshold. The background is plotted as a blue line in Fig. 1. The background regions typically look like

$$\texttt{bg}(x) = \texttt{bcx}\cdot \exp(-(x - \texttt{ex})\cdot\texttt{bsx}) \tag{8}$$

with `ex` being the position parameter for the dominant peak in the region, `bcx` and `bsx` are the background fit parameter.

4.2 Gauss peaks

Lines in the spectrum are fitted to Gauss curves

$$\texttt{peak}(a, e, s,\ x) = a \exp(-\frac{(x-e)^2}{2s^2}). \tag{9}$$

4.2.1 Conversion-e^-

The six conversion electron lines all have individual amplitude parameters `a1` . . . `a6`. The two groups each have one σ-parameter, `s` and `s4`. There are three peak position parameters `e1`, `e2`, and `e4`. The 976 keV+ group lines share a single parameter `e4`, that is scaled by the nominal peak energies. The

parameter `e1` is the position of the 482 keV peak, while the L/M doublet share parameter `e2`.

For example, the function for the 976 keV+ group of peaks is:

$$\begin{aligned} \texttt{peaks4}(x) &= \texttt{peak}(0.00703{\cdot}\texttt{a4}, \texttt{e4}{\cdot}E_{\mathrm{K2}}, \texttt{s4},\ x) \\ &+ \texttt{peak}(0.00184{\cdot}\texttt{a5}, \texttt{e4}{\cdot}E_{\mathrm{L2}}, \texttt{s4},\ x) \\ &+ \texttt{peak}(0.00054{\cdot}\texttt{a6}, \texttt{e4}{\cdot}E_{\mathrm{M2}}, \texttt{s4},\ x) \\ &+ 0.1. \end{aligned} \tag{10}$$

The constant pedestal of 0.1 prevents Gnuplot from autoscaling gazillions of decades.

4.2.2 X-rays

The X-ray lines share a position and σ-parameter, `eg` and `sg`. There are two amplitude parameters `ag1` and `ag2` for the 75 keV and the 85 keV groups. The Compton amplitudes are parametrized as ratios to the photo peak amplitudes, `agc` and `agb` for the direct Compton and the backscatter ratios. The direct Compton lines have their own position parameter `egc`.

4.2.3 Auger peak

The Auger electrons make a wide peak, parametrized with `aA`, `eA`, and `sA`.

4.3 Landau peak

The minimally ionizing electrons peak is modeled with an approximation of the Landau distribution

$$\begin{aligned} \texttt{landau}(\gamma) &= \sqrt{\frac{\exp(-\gamma - \exp(-\gamma))}{2\pi}} \\ \texttt{specl}(x) &= \texttt{al}{\cdot}\,\texttt{landau}\left(\frac{x - \texttt{el}}{\texttt{sl}}\right) \\ &+ \texttt{auger}(x) + \texttt{peaksg}(x) + \texttt{bgl}(x) \end{aligned} \tag{11}$$

with parameters `al`, `el`, and `sl`.

5 Results

5.1 Conversion electrons

Figs. 8 and 9 are closeups of the conversion electron line fits. The spectrum is drawn in green, the fitted model in black, the background in blue, and the

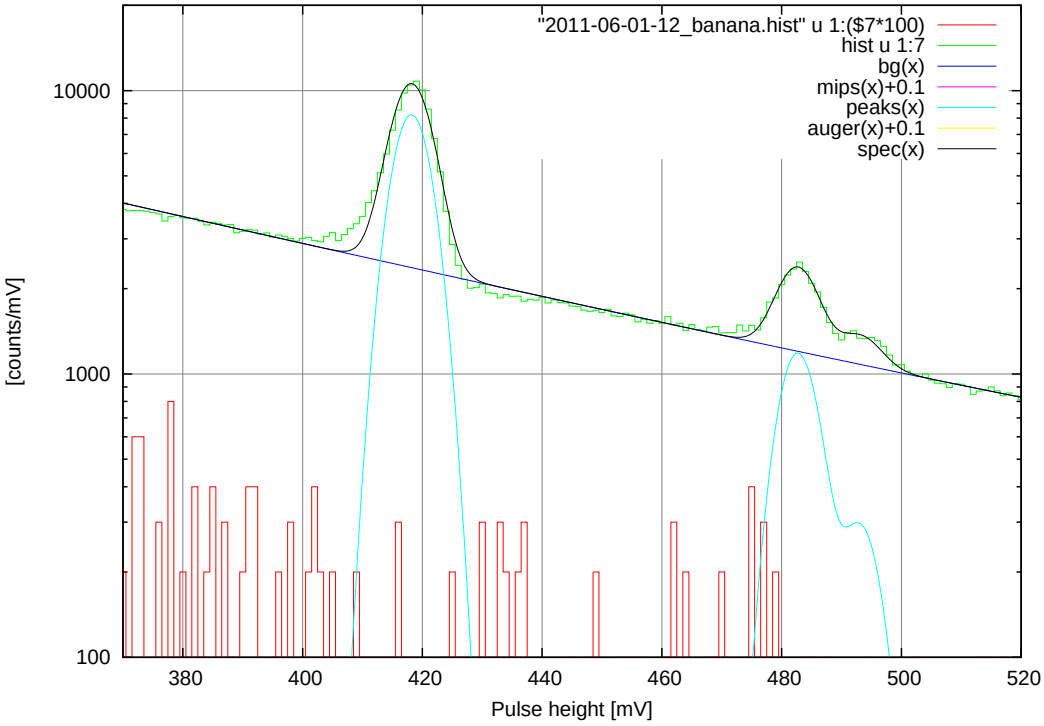

Figure 8: Zoom on the 482 keV+ conversion electron lines.

peaks in light blue. The fit results are listed in table 2.

5.1.1 Energy calibration

The peak positions are fitted directly in units of mV/keV. The two K-line calibrations differ slightly by

$$\Delta\text{cal} = \frac{\texttt{e4} - \texttt{e1}}{\texttt{e4}} = 0.7\,\%. \tag{12}$$

The DIRENA algorithm is fundamentally linear, so we can assume this difference is significant, and arises from energy loss in the air. ESTAR (NIST) provides $\mathrm{d}E/(\varrho \mathrm{d}x)$ for electrons in dry air as in table 3.

k is the true energy calibration, in mV/keV, and d is the amount of air between source and detector. By equating the measured pulse height with the expected pulse heights we get a system of linear equations

$$\texttt{e1}\cdot E_{\mathrm{K1}} = kE_{\mathrm{K1}} - kd\left(\frac{\mathrm{d}E}{\varrho \mathrm{d}x}\right)_{\mathrm{K1}} \tag{13}$$

$$\texttt{e4}\cdot E_{\mathrm{K2}} = kE_{\mathrm{K2}} - kd\left(\frac{\mathrm{d}E}{\varrho \mathrm{d}x}\right)_{\mathrm{K2}} \tag{14}$$

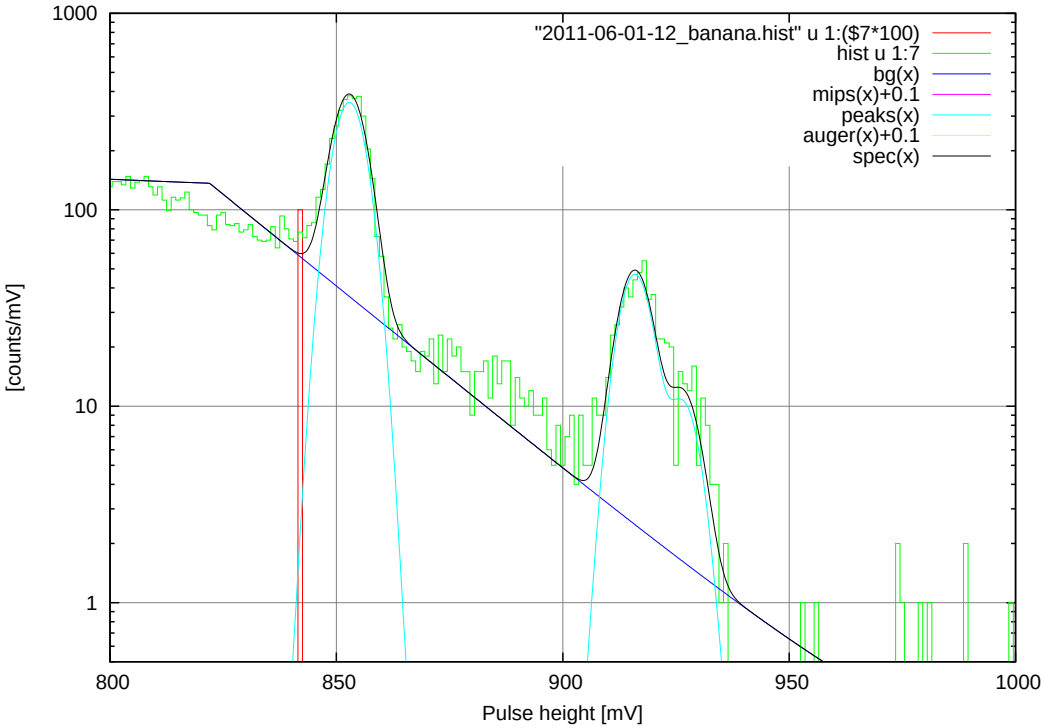

Figure 9: Zoom on the 976 keV+ conversion electron lines.

with the unknowns k and kd. The solutions are

$$k = \frac{\mathtt{e4}\cdot E_{\mathrm{K2}}\left(\frac{\mathrm{d}E}{\varrho \mathrm{d}x}\right)_{\mathrm{K1}} - \mathtt{e1}\cdot E_{\mathrm{K1}}\left(\frac{\mathrm{d}E}{\varrho \mathrm{d}x}\right)_{\mathrm{K2}}}{\left(\frac{\mathrm{d}E}{\varrho \mathrm{d}x}\right)_{\mathrm{K1}} E_{\mathrm{K2}} - \left(\frac{\mathrm{d}E}{\varrho \mathrm{d}x}\right)_{\mathrm{K2}} E_{\mathrm{K1}}} \tag{15}$$

$$dk = \frac{E_{\mathrm{K1}}E_{\mathrm{K2}}\cdot(\mathtt{e4}-\mathtt{e1})}{\left(\frac{\mathrm{d}E}{\varrho \mathrm{d}x}\right)_{\mathrm{K1}} E_{\mathrm{K2}} - \left(\frac{\mathrm{d}E}{\varrho \mathrm{d}x}\right)_{\mathrm{K2}} E_{\mathrm{K1}}} \tag{16}$$

$$d = \frac{E_{\mathrm{K1}}E_{\mathrm{K2}}\cdot(\mathtt{e4}-\mathtt{e1})}{\mathtt{e4}\cdot E_{\mathrm{K2}}\left(\frac{\mathrm{d}E}{\varrho \mathrm{d}x}\right)_{\mathrm{K1}} - \mathtt{e1}\cdot E_{\mathrm{K1}}\left(\frac{\mathrm{d}E}{\varrho \mathrm{d}x}\right)_{\mathrm{K2}}} \tag{17}$$

With the numbers from table 3, we can estimate the distance in air a

$$\begin{aligned} k &= \frac{(0.8742\cdot 975.7\cdot 1823 - 0.8682\cdot 481.7\cdot 1675)\,\mathrm{mV\,keV\,cm^2/g}}{(975.7\cdot 1823 - 481.7\cdot 1675)\,\mathrm{keV^2\,cm^2/g}} \\ &= (0.87913 \pm 0.00012)\,\mathrm{mV/keV} \end{aligned} \tag{18}$$

$$\begin{aligned} d &= \frac{975.7\cdot 481.7\cdot (0.8742 - 0.8682)\,\mathrm{mV^2\,keV}}{(0.8742\cdot 975.7\cdot 1823 - 0.8682\cdot 481.7\cdot 1675)\,\mathrm{mV\,keV\,cm^2/g}} \\ &= (3.29 \pm 0.08)\,\mathrm{mg/cm^2} \end{aligned} \tag{19}$$

Table 2: Fit results for the conversion electron lines.

parameter	value	error	rel. error
bs1	0.01135	±0.00016	1.4 %
bc1	1603	±10	0.6 %
e1	0.86829	±0.00011	0.013 %
e2	0.87168	±0.00040	0.047 %
s	3.36	±0.05	1.5 %
a1	$3.84{\cdot}10^6$	$\pm 0.07{\cdot}10^6$	1.7 %
a2	$1.92{\cdot}10^6$	$\pm 0.10{\cdot}10^6$	5 %
a3	$1.39{\cdot}10^6$	$\pm 0.24{\cdot}10^6$	17 %
bc4	25.0	±1.0	4 %
bs4	0.0437	±0.0018	4 %
e4	0.87424	±0.00011	0.013 %
s4	3.42	±0.10	2.8 %
a4	36000	±1300	4 %
a5	18000	±1500	9 %
a6	14300	±2800	20 %

Table 3: Energy loss of e^- in dry air, by ESTAR.

line	E[keV]	$\frac{\mathrm{d}E}{\varrho \mathrm{d}x}[\frac{\mathrm{MeV}}{\mathrm{g/cm^2}}]$
AU	56.7	5.322
K1	481.7	1.823
L1	553.8	1.774
M1	565.8	1.768
K2	975.7	1.675
L2	1048	1.672
M2	1060	1.671

$$a \;=\; \frac{d}{\varrho_{\mathrm{air}}} = \frac{3.3\,\mathrm{mg/cm^2}}{1.2\,\mathrm{mg/cm^3}} = 2.8\,\mathrm{cm}. \tag{20}$$

The errors are only from the fit. No systematic errors were considered. I am pretty sure that the real distance was more than $a = 3\,\mathrm{cm}$.

5.1.2 Electron energy resolution

The width σ of the 482 keV-peak is

$$\sigma_{482} = \frac{\mathtt{s}}{k} = \frac{3.35\,\mathrm{mV}}{0.879\,\mathrm{mV/keV}} = (3.81 \pm 0.06)\,\mathrm{keV}. \tag{21}$$

The resolution of the 976 keV-peak is slightly worse, but not significantly

$$\sigma_{976} = \frac{\texttt{s4}}{k} = \frac{3.41\,\mathrm{mV}}{0.879\,\mathrm{mV/keV}} = (3.88 \pm 0.11)\,\mathrm{keV}. \tag{22}$$

The FWHM is

$$W_{482} = \sqrt{\ln 256}\sigma_{482} = (8.97 \pm 0.14)\,\mathrm{keV} \tag{23}$$

The energy resolution is probably dominated by the energy loss straggling in the air.

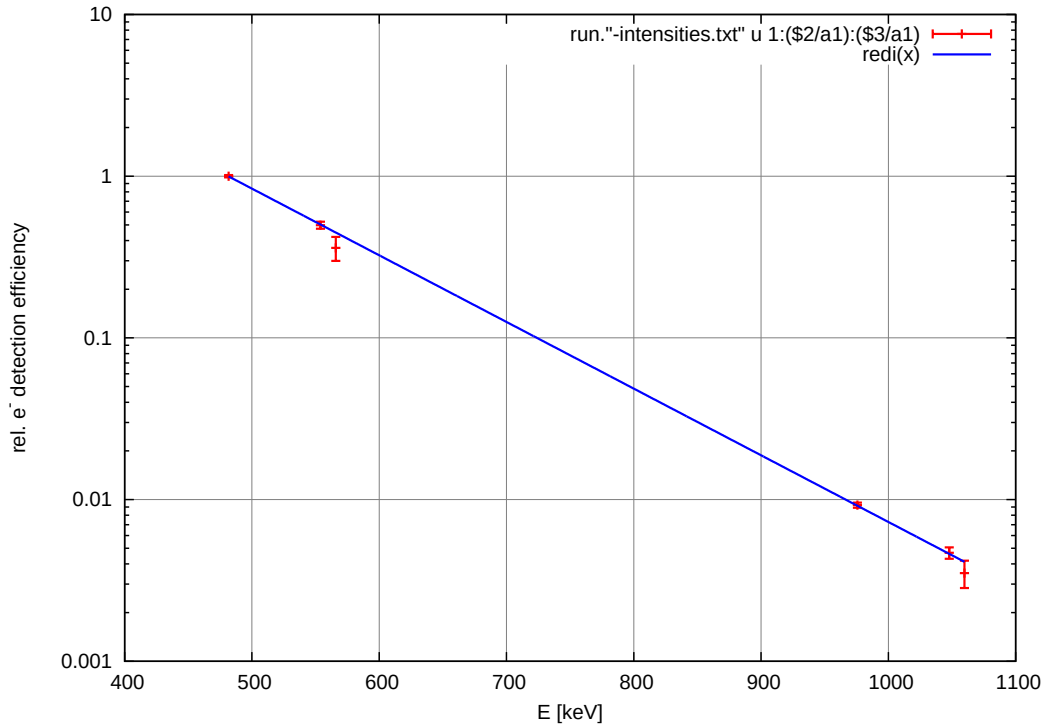

Figure 10: Relative absorption efficiency vs electron energy, normalized to the 482 keV-line.

5.1.3 Electron absorption efficiency

The amplitude parameters are scaled in the model formulas by the line intensities. If all the absorption probabilities were the same, those parameters should have the same value. In Fig. 10, the y-axis are the fitted peak heights normalized to the 482 keV-peak, scaled by the emission line intensities.

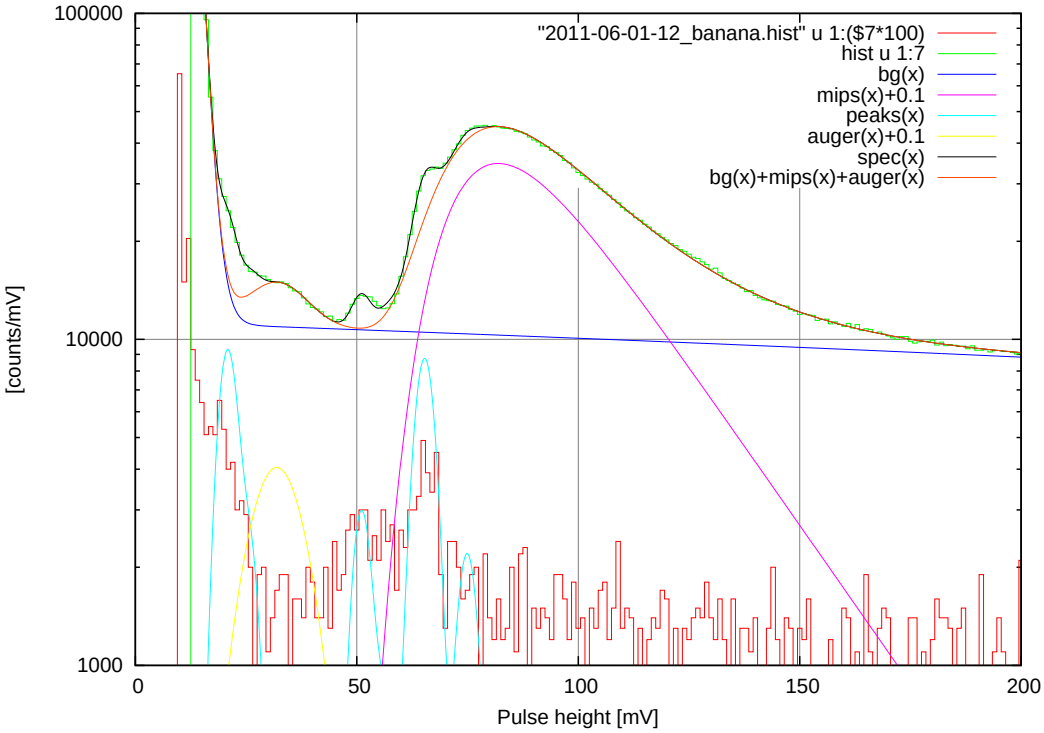

Figure 11: Zoom on the X-ray lines.

5.2 X-rays

Fig. 11 is a closer look at the MIPS peak, the Auger electron signal, and the X-rays. The pink curve is the Landau model of the minimally ionizing particle peak. The yellow curve is the Gauss-peak model of the Auger electrons. The orange curve is everything but the X-ray peaks. Table 4 lists the fit results.

5.2.1 Background

The Landau peak sits on top of a linear background, caused by all those slower electrons that pass the detector. The trigger at 12 mV probably hits the tail of the photo peak of the intense X-ray line at 10.6 keV. This is modeled by an exponential background. The sum of both background models is drawn in blue in Fig. 11.

5.2.2 Landau peak

The Landau (and the Auger-) peak basically just models more background for the X-ray lines. Nevertheless, the parameters may yield some physical

Table 4: Fit results for the low energy region.

parameter	value	error	rel. error
bc0	266400	±1000	0.4 %
bs0	0.6381	±0.0039	0.6 %
bcl	9620	±190	2.0 %
bsl	0.00117	±0.00011	10 %
ag1	13800	±1700	12 %
ag2	15100	±620	4 %
agc	0.94	±0.05	5 %
agb	0.31	±0.03	10 %
eg	0.8800	±0.0009	0.10 %
sg	2.10	±0.07	3.29 %
egc	1.221	±0.007	0.5 %
aA	$1.25{\cdot}10^6$	$\pm 0.07{\cdot}10^6$	6 %
eA	0.560	±0.009	1.6 %
sA	6.6	±0.6	9 %
al	127800	±700	0.5 %
el	81.94	±0.10	0.13 %
sl	11.16	±0.07	0.6 %

insight. The most probable energy loss is

$$E_{mp} = \frac{\texttt{el}}{k} = \frac{81.94\,\mathrm{mV}}{0.879\,\mathrm{mV/keV}} = 93.2\,\mathrm{keV} \tag{24}$$

The width parameter yields

$$\sigma = \frac{\texttt{sl}}{k} = \frac{11.16\,\mathrm{mV}}{0.879\,\mathrm{mV/keV}} = 12.7\,\mathrm{keV} \tag{25}$$

Somebody may be able to calculate the mean energy loss from these numbers, and match them to the ESTAR result for 976 keV electrons

$$\frac{\mathrm{d}E}{\varrho \mathrm{d}x}_{\mathrm{Si}}(976\,\mathrm{keV}) = 1.532\,\mathrm{MeV/g\,cm^2} \tag{26}$$

Assuming the detectors are $w = 300\,\mu$m thick, the mean energy loss should be

$$\Delta E = w\varrho_{\mathrm{Si}}\frac{\mathrm{d}E}{\varrho \mathrm{d}x}_{\mathrm{Si}}(976\,\mathrm{keV}) = 300\,\mu\mathrm{m}{\cdot}2.330\,\mathrm{g/cm^3}{\cdot}1.532\,\mathrm{MeV/g\,cm^2} = 107\,\mathrm{keV} \tag{27}$$

5.2.3 Auger e^-

The Auger electron peak is located at

$$E_{d,\mathrm{Au}} = \frac{\mathtt{eA}}{k} \cdot E_{\mathrm{Au}} = \frac{0.560\,\mathrm{mV/keV}}{0.879\,\mathrm{mV/keV}} \cdot 56.7\,\mathrm{keV} = 36.1\,\mathrm{keV} \tag{28}$$

with a width of

$$\sigma_{d,\mathrm{Au}} = \frac{\mathtt{sA}}{k} = \frac{6.6\,\mathrm{mV}}{0.879\,\mathrm{mV/keV}} = 7.5\,\mathrm{keV} \tag{29}$$

Using the energy loss from ESTAR for 56.7 keV electrons in dry air, the detector source distance would be $a = 3.2\,\mathrm{cm}$, which matches the estimate from the conversion electrons in section 5.1.1. This estimate does not take into account that the electron slows down substantially, and thus looses more energy the farther it goes.

5.2.4 Photo peaks

Two X-ray photo peaks are visible in the spectrum. These are fitted to a total of five Gauss peaks, with their intensities with each group fixed according to table 1. There is only one position parameter, which puts the calibration at

$$\mathtt{eg} = (0.8800 \pm 0.0009)\,\mathrm{mV/keV}, \tag{30}$$

in very nice agreement with the electron calibration Eq. 18,

$$k = (0.87913 \pm 0.00012)\,\mathrm{mV/keV} \tag{31}$$

All X-ray lines share a single width parameter, which yields a resolution

$$\sigma_\gamma = \frac{\mathtt{sg}}{k} = \frac{2.10\,\mathrm{mV}}{0.879\,\mathrm{mV/keV}} = 2.4\,\mathrm{keV}. \tag{32}$$

This is a lot better than the electron resolution, possibly because the γs do not straggle in the air.

The relative amplitudes of the X-rays around 75 keV vs 85 keV is

$$\frac{\mathtt{ag2}}{\mathtt{ag2}} = \frac{15100}{13800} = 1.10 \pm 0.13. \tag{33}$$

That is not a significant difference, although we expect that 75 keV γs are slightly more probable to do photoeffect than 85 keV γs, and the measured ratio seems to support that.

5.2.5 Compton backscatter

The backscatter peak is nicely isolated at 51 mV and probably contributes the most to the fit accuracy.

The ratio of backscatter intensity compared to the photo peak is

$$\texttt{agb} = 0.31 \pm 0.03. \tag{34}$$

That is the only fit parameter that is independent of the photo peak models.

5.2.6 Compton peak

The direct Compton peak is almost hidden by background. The fit treats the peak pretty freely with two parameters, the intensity ratio compared to the photo peak

$$\texttt{agc} = 0.94 \pm 0.05, \tag{35}$$

and a position that comes out offset by a factor

$$\frac{\texttt{egc}}{\texttt{eg}} = \frac{1.221}{0.8800} = 1.4. \tag{36}$$

This is mostly filling in the background, but is is there.

The red spectrum in Fig. 11 show X-ray peaks with much reduced electron background, because the source was outside the box. The direct Compton peak appears at the correct position. I am going to take more data in that mode.

6 Conclusion

The IRENA is capable to capture signals of a good preamp with good resolution and high dynamic range, both in energy and in intensity.

The IRENA can read nine dual gain channels in simultaneously in coincidence, but that was not tested in this study. With multi channel readout, some care must be taken with signal which are wider out of phase, and multiple triggers for the same event.

A ^{207}Bi-source is a marvelous tools for testing and calibrating silicon detectors and readout electronics.

This paper is meant as a guide how to go about such work.

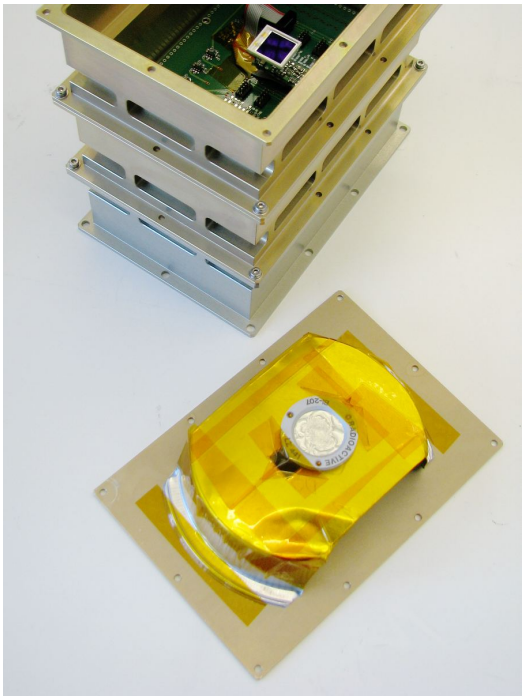

Figure 12: Source fixation for closer distance.

7 Follow up

After completion of this analysis, a second run was performed with a much reduced distance between source and detector. Fig, 12 shows how the source was fixed. Fig. 13 is the resulting spectrum. The spectrum has better resolution for the conversion and Auger electrons, and more pronounced γ-peaks.

8 References

GIYF: `http://www.giyf.com`

NuDat2: `http://www.nndc.bnl.gov/nudat2`

ESTAR: `http://physics.nist.gov/PhysRefData/Star/Text/ESTAR.html`

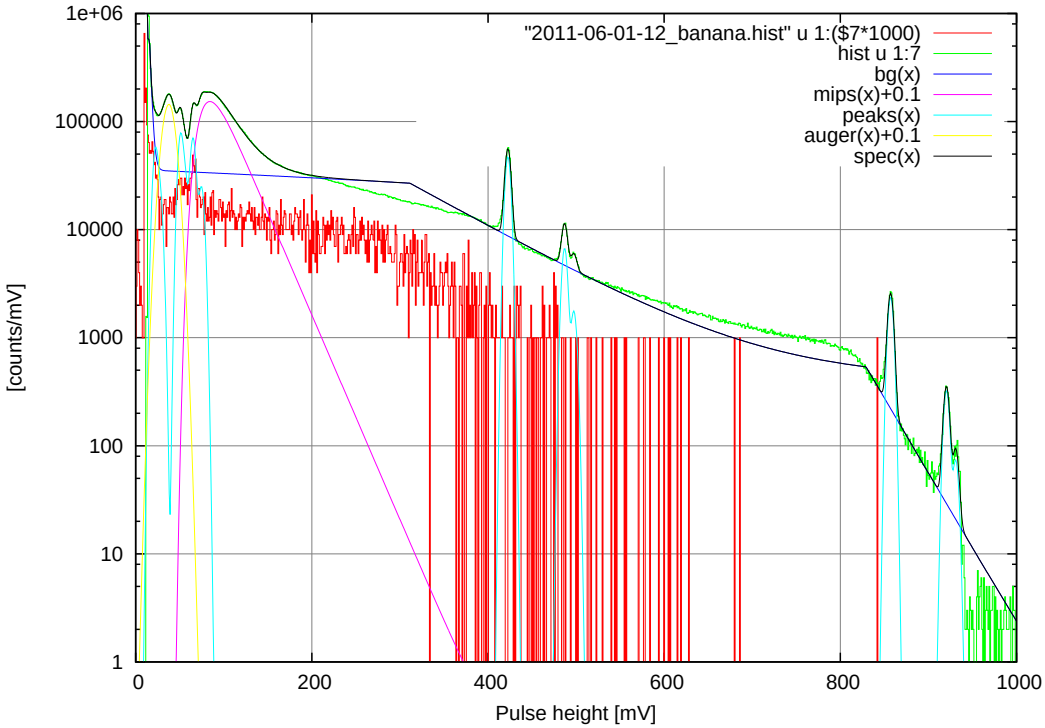

Figure 13: ^{207}Bi spectrum in 300 μm Silicon with backscatter.

9 Gnuplot script

```
# -*- gnuplot -*-
set fit errorvar

run="2011-06-01-Bi207-13"
grun="2011-06-06-Bi207-g-26"
hist=run."_banana.hist"

keV_AU = 56.7
keV_M1=565.8473
keV_L1=553.8372
keV_K1=481.6935
keV_M2=1059.805
keV_L2=1047.795
keV_K2=975.651

x0 =  14.0
x1 = 370.0
x4 = 830.0
peak(a,e,s, x)=a*exp(-((x-e)/s)**2/2)
landau(l)=sqrt(exp(-l-exp(-l))/2/pi)
mips(x)=al*landau((x-el)/sl)
bg0(x)=bc0*exp(-bs0*(x-x0))
bgl(x)=bcl*(1-bsl*(x-45.0)) + bg0(x)
bg1(x)=bc1*(exp(-bs1*(x-e1*keV_K1))+0.05)
bg4(x)=bc4*exp(-bs4*(x-e4*keV_K2))+0.1
photo0(x)=peak(ag0*0.332, eg*10.6, sg, x)
photo2(x)=peak(ag2*0.214, eg*72.805, sg, x)+peak(ag2*0.357, eg*74.969, sg, x)
photo1(x)=peak(ag1*0.0827,eg*84.938, sg, x)+peak(ag1*0.0431,eg*84.45, sg, x)+peak(ag1*0.0302,eg*87.3, sg, x)
comptonb(x)=peak(agb*ag1*0.156, eg*64, sg, x)+peak(agb*ag2*0.57, eg*58, sg, x)
comptonc(x)=peak(agc*ag1*0.156, egc*21, sg, x)+peak(agc*ag2*0.57, egc*17, sg, x)
auger(x)=peak(0.0029*aA,eA*keV_AU,sA, x)
peaksg(x)=photo1(x)+photo2(x)+comptonb(x)+comptonc(x)
specl(x)=bgl(x)+mips(x)+auger(x)+peaksg(x)
peaks1(x)=peak(0.001515*a1,e1*keV_K1,s, x)+peak(0.000438*a2,e2*keV_L1,s, x)+peak(0.000147*a3,e2*keV_M1,s, x)
spec1(x)=bg1(x)+peaks1(x)
peaks4(x)=peak(0.00703*a4,e4*keV_K2,s4, x)+peak(0.00184*a5,e4*keV_L2,s4, x)+peak(0.00054*a6,e4*keV_M2,s4, x)
spec4(x)=bg4(x)+peaks4(x)
spec(x)= x<x0 ? bg0(x0) : (x<x1 && bgl(x)<bg1(x)) ? specl(x) : (x<x4 && bg1(x)<bg4(x)) ? spec1(x) : spec4(x)
bg(x) =  x<x0 ? bg0(x0) : (x<x1 && bgl(x)<bg1(x)) ? bgl(x)   : (x<x4 && bg1(x)<bg4(x)) ? bg1(x)   : bg4(x)
peaks(x)=peaksg(x)+peaks1(x)+peaks4(x)+0.1

bs1             = 0.0110981        # ±  0.0001644    (1.481%)
bc1             = 2261.94          # ±  14.47        (0.6397%)
a1              = 5.30208e+06      # ±  9.475e+04    (1.787%)
e1              = 0.868076         # ±  0.0001209    (0.01392%)
s               = 3.40574          # ±  0.05283      (1.551%)
a2              = 2.38026e+06      # ±  1.394e+05    (5.859%)
e2              = 0.871619         # ±  0.0004794    (0.055%)
a3              = 1.02883e+06      # ±  3.454e+05    (33.57%)

bc4             = 36.0099          # ±  1.383        (3.84%)
bs4             = 0.0429582        # ±  0.001575     (3.666%)
a4              = 50038.5          # ±  1790         (3.577%)
a5              = 25377.7          # ±  2049         (8.074%)
a6              = 18795.1          # ±  3636         (19.35%)
e4              = 0.874142         # ±  0.0001079    (0.01235%)
s4              = 3.40073          # ±  0.09327      (2.743%)

bc0             = 297892           # ±  1136         (0.3813%)
ag1             = 15198.3          # ±  1838         (12.09%)
ag2             = 16833.9          # ±  677.2        (4.023%)
aA              = 1.3905e+06       # ±  7.758e+04    (5.579%)
al              = 142804           # ±  715.4        (0.501%)
bcl             = 10752.5          # ±  206.8        (1.924%)
bsl             = 0.00116955       # ±  0.0001106    (9.454%)
el              = 81.9202          # ±  0.0996       (0.1216%)
sl              = 11.1467          # ±  0.07011      (0.629%)
agc             = 0.951017         # ±  0.04764      (5.009%)
agb             = 0.308091         # ±  0.03127      (10.15%)
eg              = 0.879913         # ±  0.0008749    (0.09943%)
sg              = 2.09985          # ±  0.06708      (3.194%)
sA              = 6.52275          # ±  0.5671       (8.694%)
eA              = 0.562325         # ±  0.008591     (1.528%)
egc             = 1.22231          # ±  0.006272     (0.5131%)
bs0             = 0.636961         # ±  0.003771     (0.5921%)

set autoscale
set style data histeps
set grid lt 9
set log y
set samples 1000
```

```
set xra [x1:520]
plot grun."_banana.hist" u 1:7, hist u 1:7, \
     bg(x), mips(x)+0.1, peaks(x), auger(x)+0.1, spec(x)

fit [x1:520] spec1(x) hist u 1:7:(sqrt($7)) via bc1
replot
fit [x1:520] spec1(x) hist u 1:7:(sqrt($7)) via a1,a2,a3
replot
fit [x1:520] spec1(x) hist u 1:7:(sqrt($7)) via bc1
replot
fit [x1:520] spec1(x) hist u 1:7:(sqrt($7)) via a1,a2,a3,bc1
replot
fit [x1:520] spec1(x) hist u 1:7:(sqrt($7)) via bs1,bc1,a1,e1,s,a2,e2,a3
replot
fit [x1:520] spec1(x) hist u 1:7:(sqrt($7)) via bs1,bc1,a1,e1,s,a2,e2,a3
replot

set xra [x4:940]
fit [x4:940] spec4(x) hist u 1:7:(sqrt($7+0.1)) via bc4
replot
fit [x4:940] spec4(x) hist u 1:7:(sqrt($7+0.1)) via a4,a5,a6
replot
fit [x4:940] spec4(x) hist u 1:7:(sqrt($7+0.1)) via bc4,bs4,a4,a5,a6
replot
fit [x4:940] spec4(x) hist u 1:7:(sqrt($7+0.1)) via bc4,bs4,a4,a5,a6,e4,s4
replot

set xra [x0:120]
fit [x0:120] specl(x) hist u 1:7:(sqrt($7+0.1)) via bc0,ag1,ag2,aA,al,bcl
replot
fit [x0:200] specl(x) hist u 1:7:(sqrt($7+0.1)) via bc0,ag1,ag2,aA,al,bcl,bsl,el,sl
replot
fit [x0:200] specl(x) hist u 1:7:(sqrt($7+0.1)) via bc0,ag1,ag2,aA,al,bcl,bsl,el,sl,agc,agb,eg,sg,sA,eA,egc,bs0
replot

set xra [0:1000]
set yra [1:1e5]
replot

#  ESTAR stopping power in Nitrogen

# 5.670E-02 5.360E+00 3.836E-03 5.364E+00
# 4.817E-01 1.828E+00 6.717E-03 1.834E+00
# 5.538E-01 1.777E+00 7.383E-03 1.785E+00
# 5.658E-01 1.770E+00 7.497E-03 1.778E+00
# 9.757E-01 1.672E+00 1.186E-02 1.684E+00
# 1.048E+00 1.668E+00 1.270E-02 1.681E+00
# 1.060E+00 1.667E+00 1.285E-02 1.680E+00

#  ESTAR stopping power in dry Air

# 5.670E-02 5.318E+00 4.046E-03 5.322E+00
# 4.817E-01 1.816E+00 7.050E-03 1.823E+00
# 5.538E-01 1.766E+00 7.746E-03 1.774E+00
# 5.658E-01 1.760E+00 7.865E-03 1.768E+00
# 9.757E-01 1.662E+00 1.242E-02 1.675E+00
# 1.048E+00 1.658E+00 1.330E-02 1.672E+00
# 1.060E+00 1.658E+00 1.345E-02 1.671E+00

dEdx1 = 1.823e3
dEdx2 = 1.774e3
dEdx4 = 1.675e3
dEdxA = 5.322e3

# e1*keV_K1 = e * keV_K1 - de * dEdx1
# e4*keV_K2 = e * keV_K2 - de * dEdx4
# eA*keV_AU = e * keV_AU - de * dEdxA

dd = dEdx1*keV_K2 - dEdx4*keV_K1
e = (e4*dEdx1*keV_K2 - e1*dEdx4*keV_K1)/dd
de = keV_K1*keV_K2*(e4-e1)/dd
d = de/e
d = keV_K1*keV_K2*(e4-e1)/(e4*dEdx1*keV_K2 - e1*dEdx4*keV_K1)

round(x,p)=int(x/p+0.5)*p

rhoAir = 1013e2*1e-6/8.3/300*29  # hPa * cm^2 / (J/mol/K) / K * g/mol = g/cm^2
print "Air thickness (K1-K2): ", round(d/rhoAir, 0.1), "cm"

#dA = (e4-eA)*keV_AU/dEdxA/e4
#ee = e4/(1-dA*dEdx4/keV_K2)
#dA = (ee-eA)*keV_AU/dEdxA/e
#ee = e4/(1-dA*dEdx4/keV_K2)
```

```
#dA = (ee-eA)*keV_AU/dEdxA/e

dA = keV_AU*keV_K2*(e4-eA)/(e4*dEdxA*keV_K2 - eA*dEdx4*keV_AU)
print "Air thickness (AU): ", round(dA/rhoAir, 0.1), "cm"

print "Energy loss AU  (57): ", round(d*dEdxA,0.01), "keV"
print "Energy loss K1 (482): ", round(d*dEdx1,0.01), "keV"
print "Energy loss L1 (554): ", round(d*dEdx2,0.01), "keV"
print "Energy loss K2 (976): ", round(d*dEdx4,0.01), "keV"

print "e_AU(057) = ", round(eA, 0.0001), " ±", round(eA_err, 0.0001), ", e(K1/K2) = ", round(eA/(1-d*dEdxA/keV_AU), 0.0001), \
      ", e(AU) = ", round(eA/(1-dA*dEdxA/keV_AU), 0.0001)
print "e_K1(482) = ", round(e1, 0.0001), " ±", round(e1_err, 0.0001), ", e(K1/K2) = ", round(e1/(1-d*dEdx1/keV_K1), 0.0001), \
      ", e(AU) = ", round(e1/(1-dA*dEdx1/keV_K1), 0.0001)
print "e_L1(554) = ", round(e2, 0.0001), " ±", round(e2_err, 0.0001), ", e(K1/K2) = ", round(e2/(1-d*dEdx2/keV_L1), 0.0001), \
      ", e(AU) = ", round(e2/(1-dA*dEdx2/keV_L1), 0.0001)
print "e_K1(976) = ", round(e4, 0.0001), " ±", round(e4_err, 0.0001), ", e(K1/K2) = ", round(e4/(1-d*dEdx4/keV_K2), 0.0001), \
      ", e(AU) = ", round(e4/(1-dA*dEdx4/keV_K2), 0.0001)
print "e_gamma   = ", round(eg, 0.0001), " ±", round(eg_err, 0.0001)

# ESTAR stopping power in Si

# 9.000E-01 1.516E+00 2.145E-02 1.537E+00 3.077E-01
# 9.757E-01 1.509E+00 2.307E-02 1.532E+00 3.340E-01
# What is that density parameter?

rhoSi = 2.330 # g/cm^2
keV_L = 0.03*rhoSi*1535

print "electron resolution ", round(s,0.01), "mV, ", round(s/e,0.01), "keV"
print "gamma resolution    ", round(sg,0.01), "mV, ", round(sg/e,0.01), "keV"

set print run."-intensities.txt"
print keV_K1, a1, a1_err
print keV_L1, a2, a2_err
print keV_M1, a3, a3_err
print keV_K2, a4, a4_err
print keV_L2, a5, a5_err
print keV_M2, a6, a6_err
unset print

set term wxt 1 enhanced
set xlab "E [keV]"
set ylab "rel. e^- detection efficiency"
redi(x)=redic*exp(-redis*(x-keV_K1))
redic=1
redis=0.00947348
set autoscale
plot run."-intensities.txt" u 1:($2/a1):($3/a1) with error lt 1 lw 3,redi(x) w l lt 3 lw 3
fit redi(x) run."-intensities.txt" u 1:($2/a1):($3/a1) via redis,redic
replot

set term post enhanced solid color
set out run."-intensities.ps"
replot
unset out

set xlab "Pulse height [mV]"
set ylab "[counts/mV]"
set xra [370:520]
set yra [100:20000]
set out run."-KLM1.ps"
plot grun."_banana.hist" u 1:7, hist u 1:7, \
     bg(x), mips(x)+0.1, peaks(x), auger(x)+0.1, spec(x)
unset out
set xra [800:1000]
set yra [0.5:1000]
set out run."-KLM2.ps"
replot
unset out

set xra [0:1000]
set yra [1:100000]
set out run."-fit.ps"
replot
unset out
set xra [0:200]
set yra [1000:100000]
set out run."-Xray.ps"
replot bg(x)+mips(x)+auger(x)
unset out
set term pop
set term pop
```

```
set xra [0:1000]
set yra [1:100000]
replot

# Air thickness (K1-K2): 2.8cm
# Air thickness (AU): 3.3cm
# Energy loss AU  (57): 17.64keV
# Energy loss K1 (482): 6.04keV
# Energy loss L1 (554): 5.88keV
# Energy loss K2 (976): 5.55keV
# e_AU(057) = 0.563 ±0.0084, e(K1/K2) = 0.8173, e(AU) = 0.8799
# e_K1(482) = 0.8681 ±0.0001, e(K1/K2) = 0.8791, e(AU) = 0.8809
# e_L1(554) = 0.8715 ±0.0004, e(K1/K2) = 0.8808, e(AU) = 0.8823
# e_K1(976) = 0.8741 ±0.0001, e(K1/K2) = 0.8791, e(AU) = 0.8799
# e_gamma   = 0.8799 ±0.0009
# electron resolution 3.36mV, 3.82keV
# gamma resolution    2.1mV, 2.39keV
```